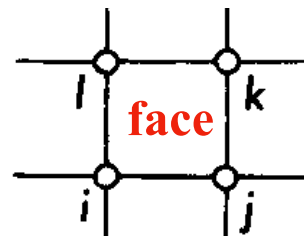


Exactly Solved Models in Statistical Mechanics (1982)

The IRF Model (Interaction-round-a-face Model)

Corner transfer matrices can be defined for any planar lattice model with finite-range interactions, but for definiteness let us consider a square lattice model with interactions round faces. For brevity I shall call this the 'IRF' model. It is defined as follows.



$$Z = \sum \prod w(\sigma_i, \sigma_j, \sigma_k, \sigma_l), \quad (13.1.2)$$

where the product is over all faces of the lattice, the sum is over all values of all the spins, and

$$w(a, b, c, d) = \exp[-\varepsilon(a, b, c, d)/k_B T]. \quad (13.1.3)$$

This $w(a, b, c, d)$ is the Boltzmann weight of the intra-face interactions between spins a, b, c, d .

Dimers on a Rectangular Lattice

R. J. BAXTER

Research School of Physical Sciences, The Australian National University, Canberra, Australia

(Received 17 July 1967)

Vertex



A set of matrix equations is derived which yields the statistical mechanical properties of a system of monomers and dimers on a rectangular lattice in the thermodynamic limit. As the matrices are strictly of infinite dimensionality, the equations cannot be solved directly, but if they are restricted to be of finite and quite small dimensionality, very good approximations to the thermodynamic properties are obtained.

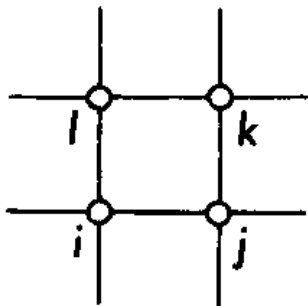
Variational Approximations for Square Lattice Models in Statistical Mechanics

R. J. Baxter¹ *Journal of Statistical Physics, Vol. 19, No. 5, 1978*

Received June 6, 1978

461

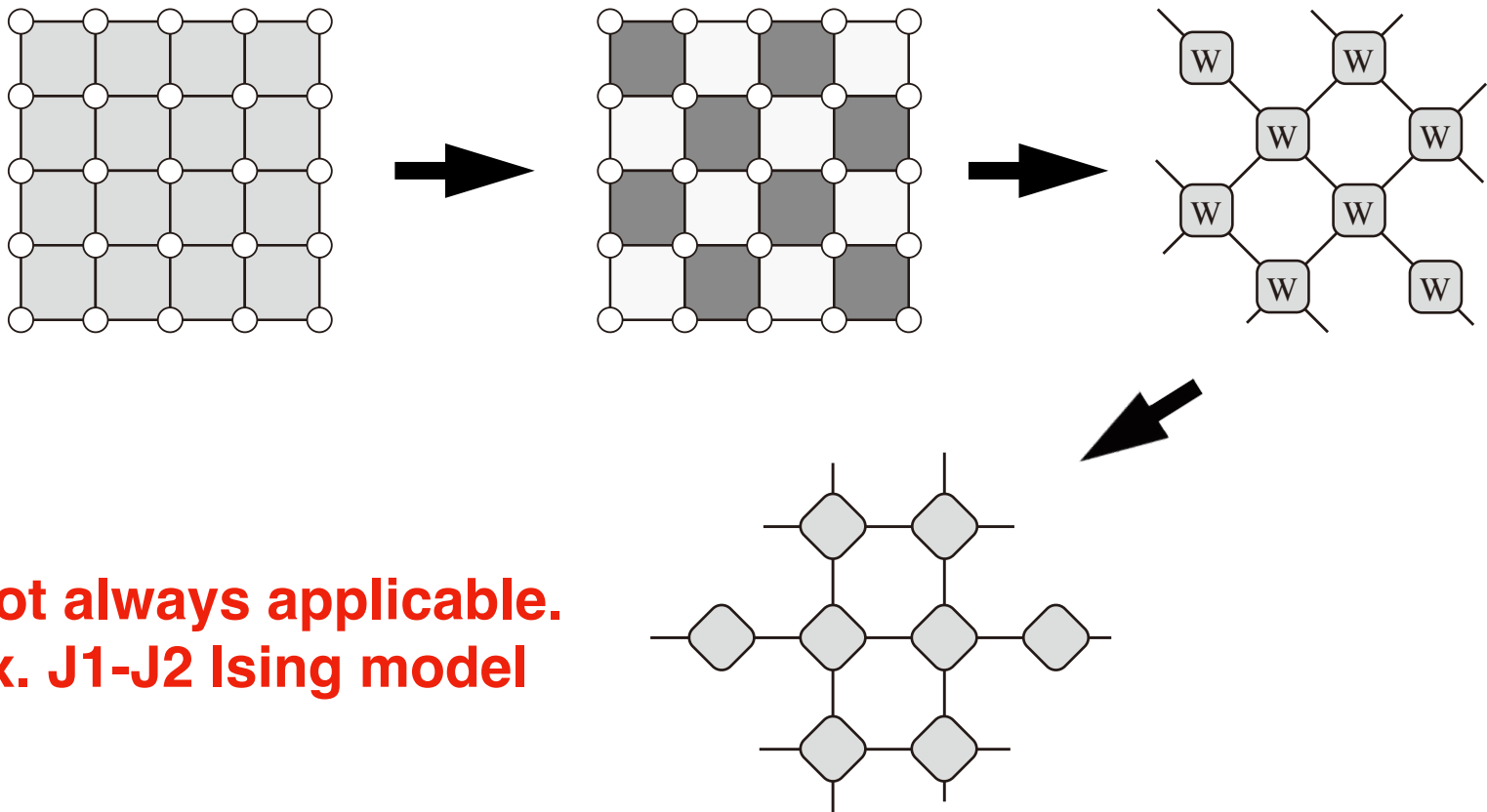
IRF



This paper concerns a square lattice, Ising-type model with interactions between the four spins at the corners of each face. These may include nearest and next-nearest-neighbor interactions, and interactions with a magnetic field. Provided the Hamiltonian is symmetric with respect to both row reversal and column reversal, a rapidly convergent sequence of variational approximations is obtained, giving the free energy and other thermodynamic properties. For the usual Ising model, the lowest such approximations are those of Bethe and of Kramers and Wannier. The method provides a new definition of corner transfer matrices.

- **Modern (2000-2024) TN formulations use the Vertex representations.**
There are several mappings from the IRF to the Vertex:

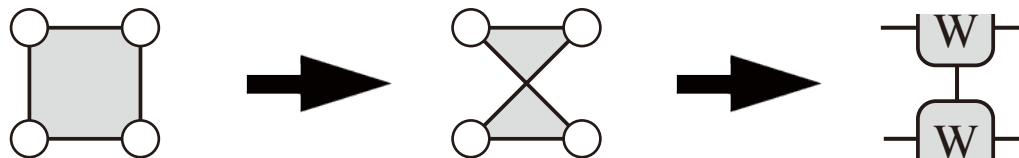
(*) When diagonal interactions are **missing**,
Chess Board type Vertex lattice naturally appears.



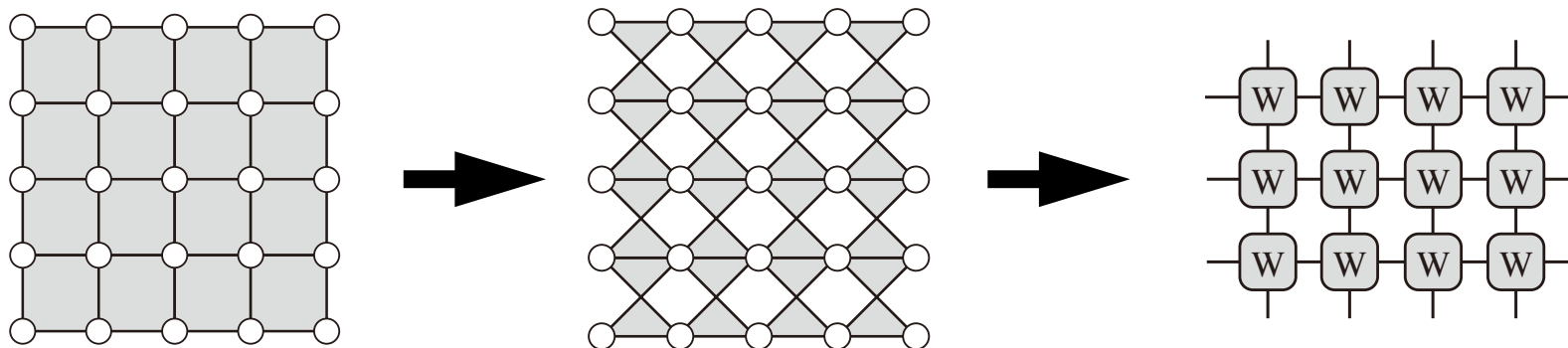
Not always applicable.
ex. J1-J2 Ising model

- **Modern (2000-2024) TN formulations use the Vertex representations.**
There are several mappings from the IRF to the Vertex:

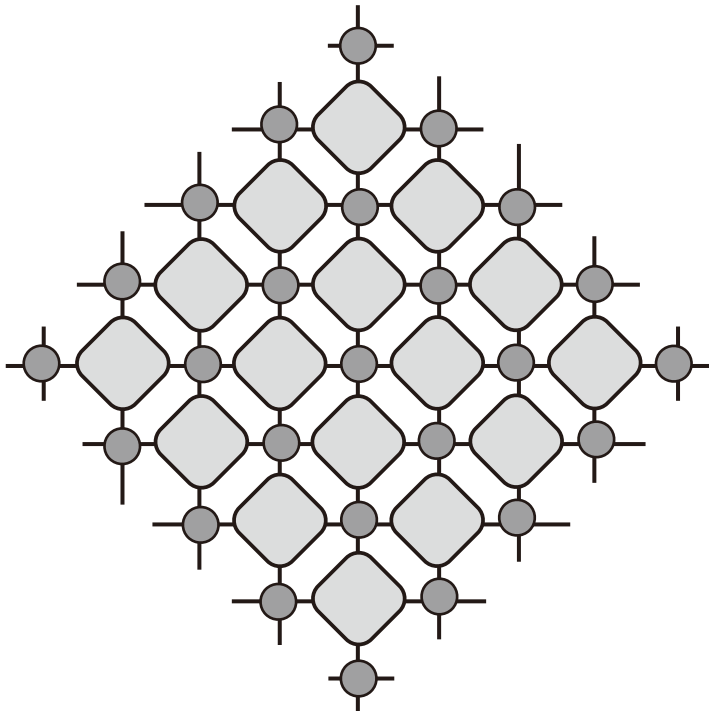
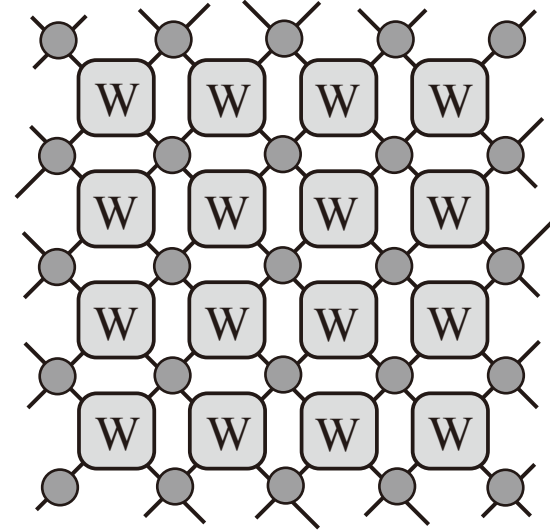
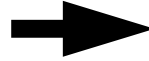
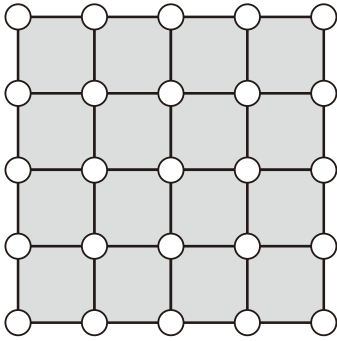
(*) via SVD, one obtains an **anisotropic** Vertex model.



on the entire lattice,



(*) Insertion of the “4-leg delta tensor” creates an anisotropic (?) vertex lattice in the diagonal direction.



$$\begin{array}{c}
 c \\
 | \\
 d - \bullet - b \\
 | \\
 a
 \end{array}
 \quad
 \delta_{ab} \delta_{bc} \delta_{cd} \delta_{da}$$

Note: There is no (?) need of performing such mapping!

Exactly Solved Models in Statistical Mechanics (1982)

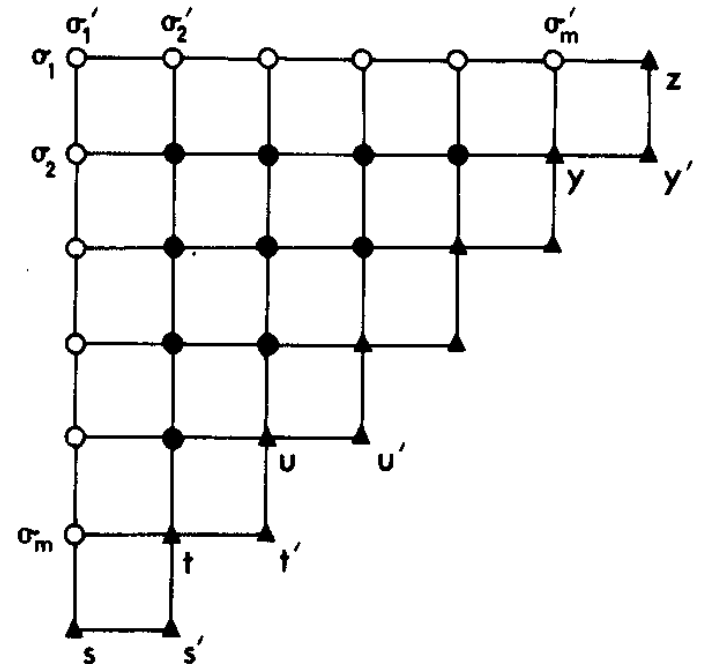
Let σ denote all the spins $\{\sigma_1, \dots, \sigma_m\}$; and σ' all the spins $\{\sigma'_1, \dots, \sigma'_m\}$. Define

$$A_{\sigma, \sigma'} = \sum \prod w(\sigma_i, \sigma_j, \sigma_k, \sigma_l) \quad \text{if } \sigma_1 = \sigma'_1, \quad (13.1.8a)$$

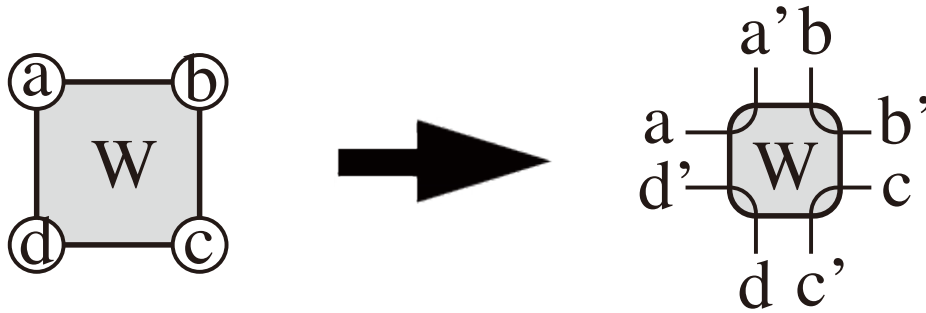
$$= 0 \quad \text{if } \sigma_1 \neq \sigma'_1, \quad (13.1.8b)$$

where the product is now over the $\frac{1}{2}m(m+1)$ faces in Fig. 13.1(b), and the sum is over all spins on sites denoted by solid circles. Note that the spins $\sigma_1, \dots, \sigma'_m$ are *not* summed over, so the RHS of (13.1.8) is a function of σ and σ' .

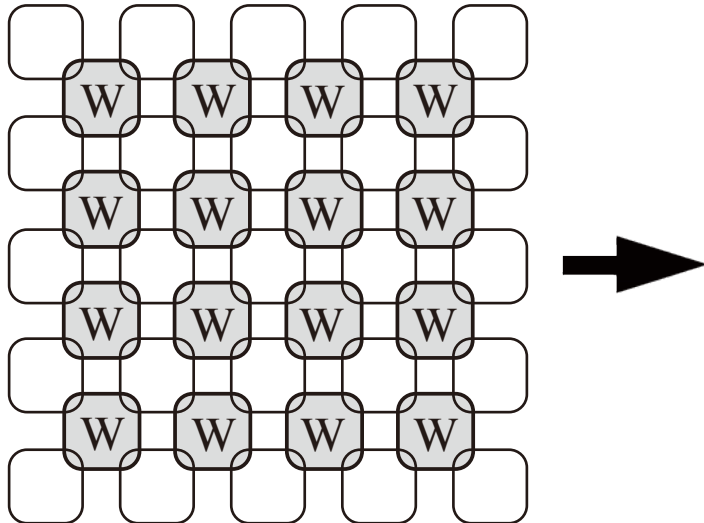
Baxter implicitly introduced 2-leg
“delta tensor” at the corner.



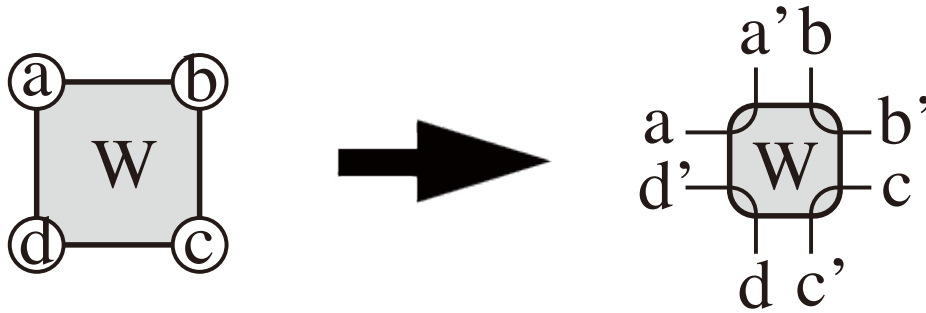
**an IRF weight can be interpreted as
a (vertex) tensor with corner double indices**



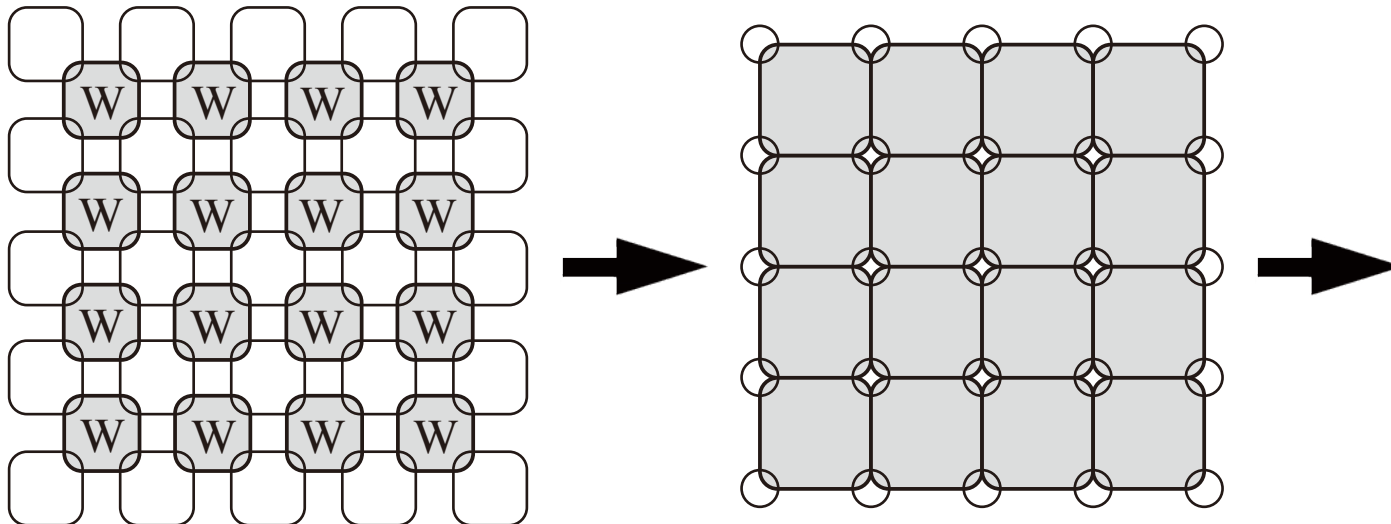
Contraction among tensors



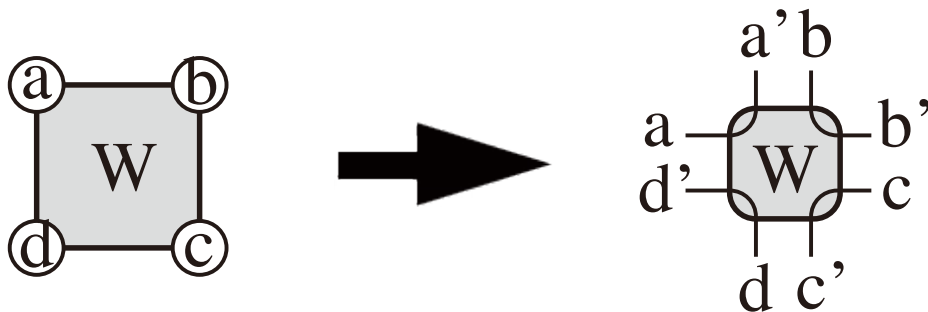
**an IRF weight can be interpreted as
a (vertex) tensor with corner double indices**



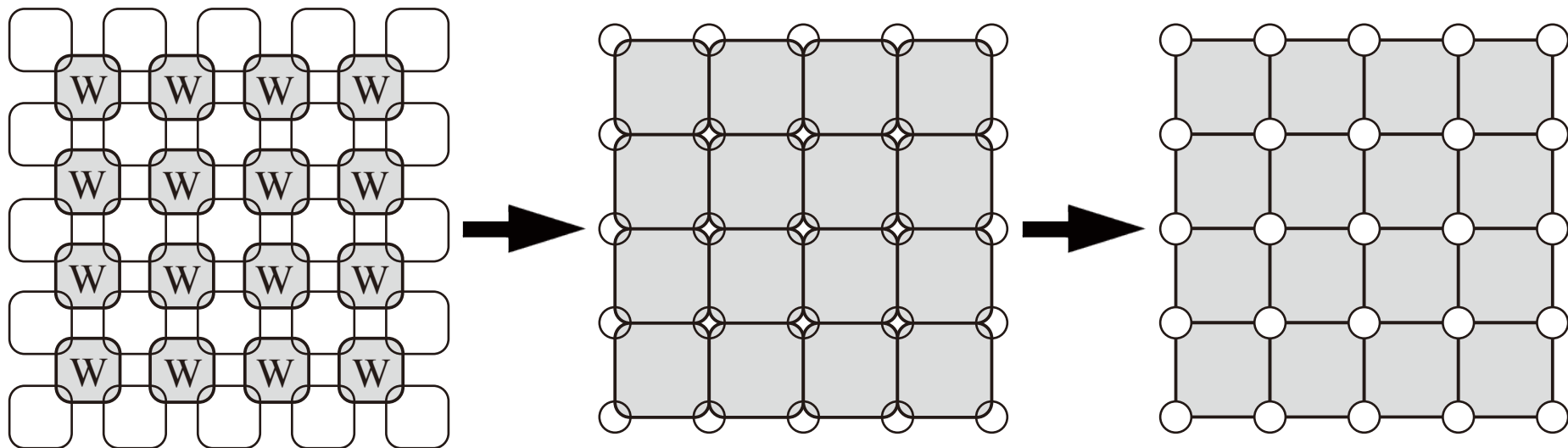
Contraction among tensors



**an IRF weight can be interpreted as
a (vertex) tensor with corner double indices**

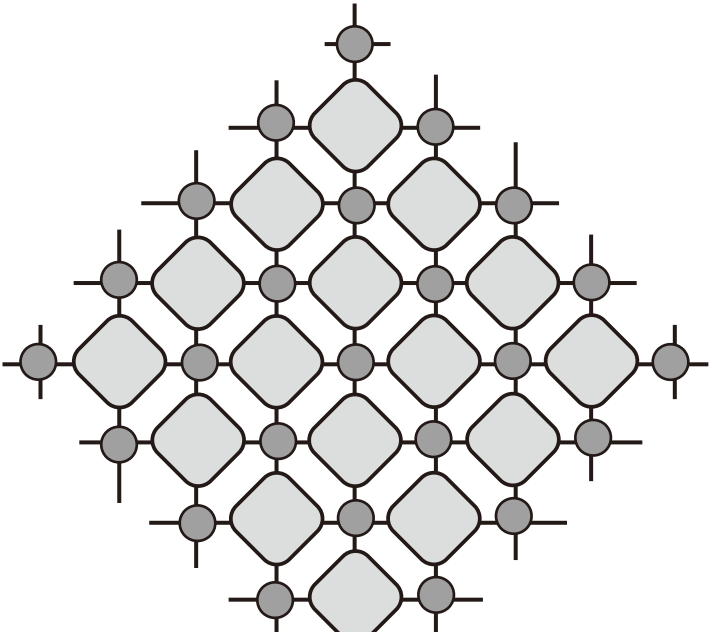
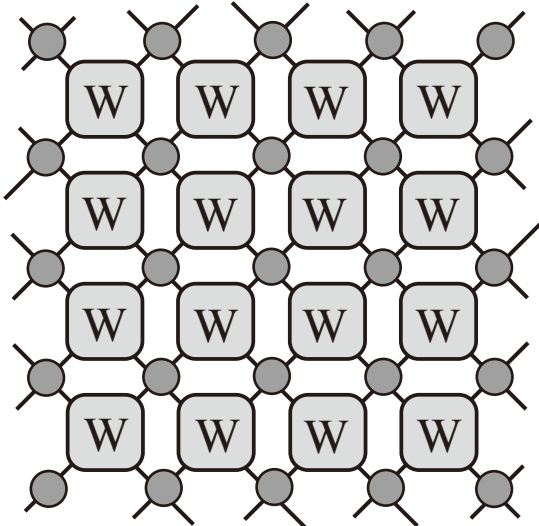
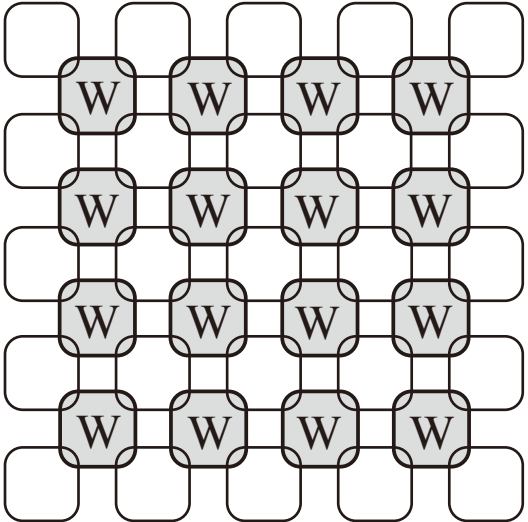


Contraction among tensors



Open circles denoted the contraction processes!!

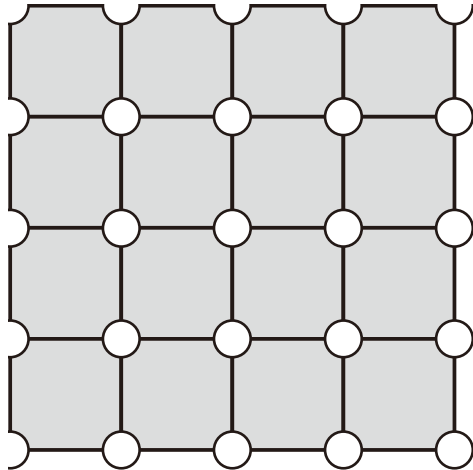
One-step application of TNR



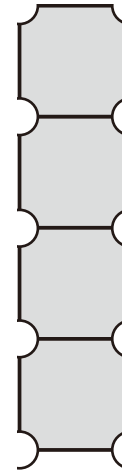
In the next step, all the delta tensors disappear (in the explicit manner).

Graphical Representations

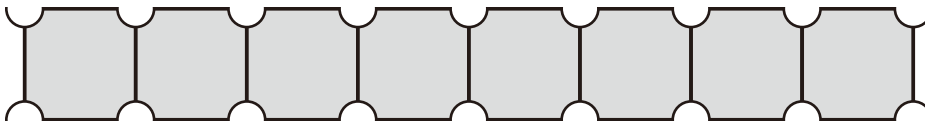
Corner Transfer Matrix (IRF)



Half-row/column TM

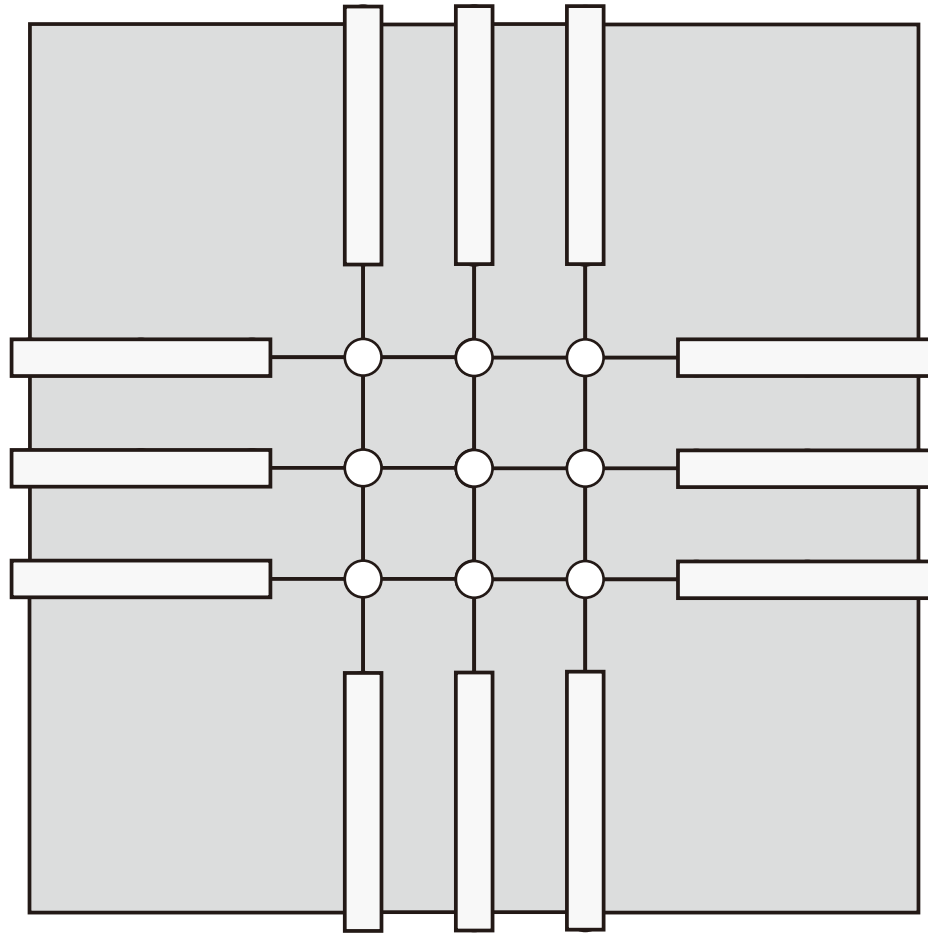


Transfer Matrix



Each double (delta) indices can be treated as single index, since they are always the same.

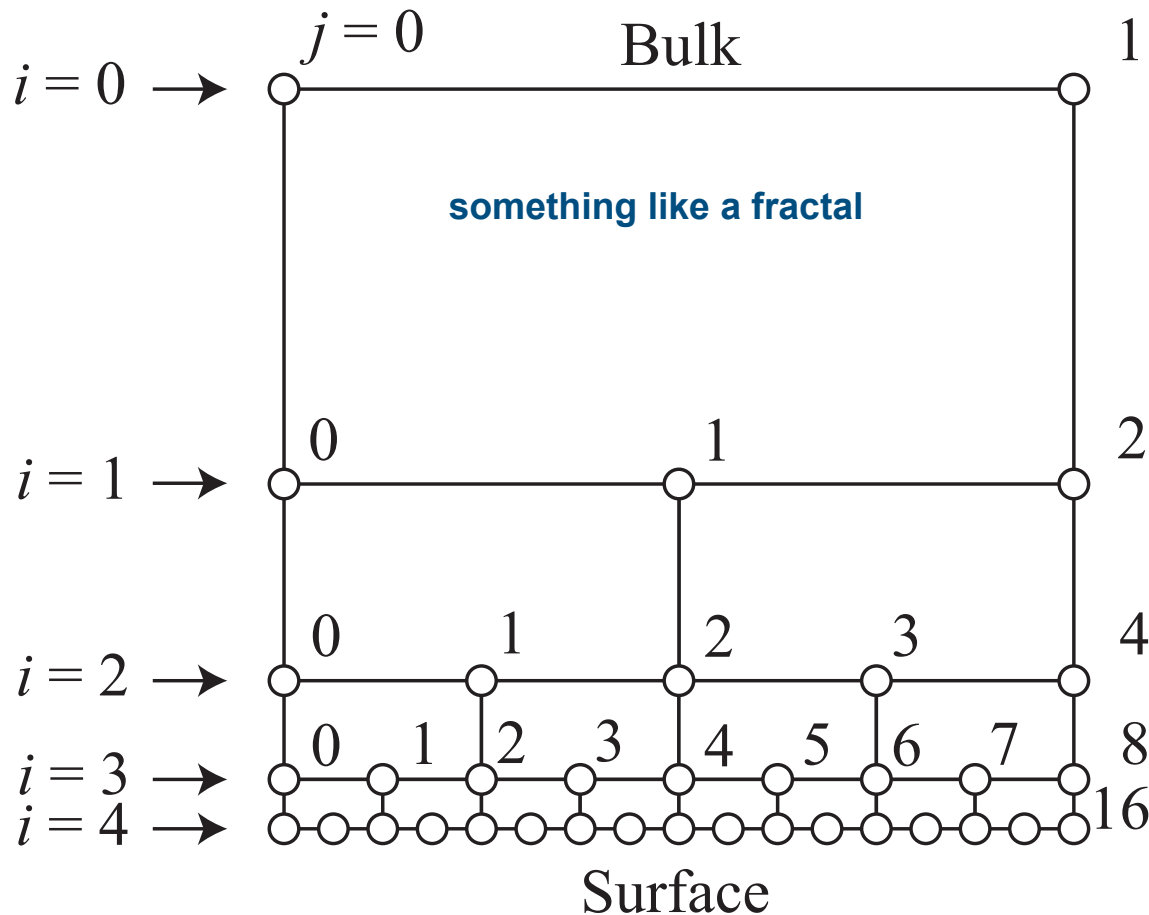
Corner Transfer Matrix RG (in IRF rep.)



do NOT to try to map the model to any on of the vertex one.

application to the **Stacked Pentagon lattice**

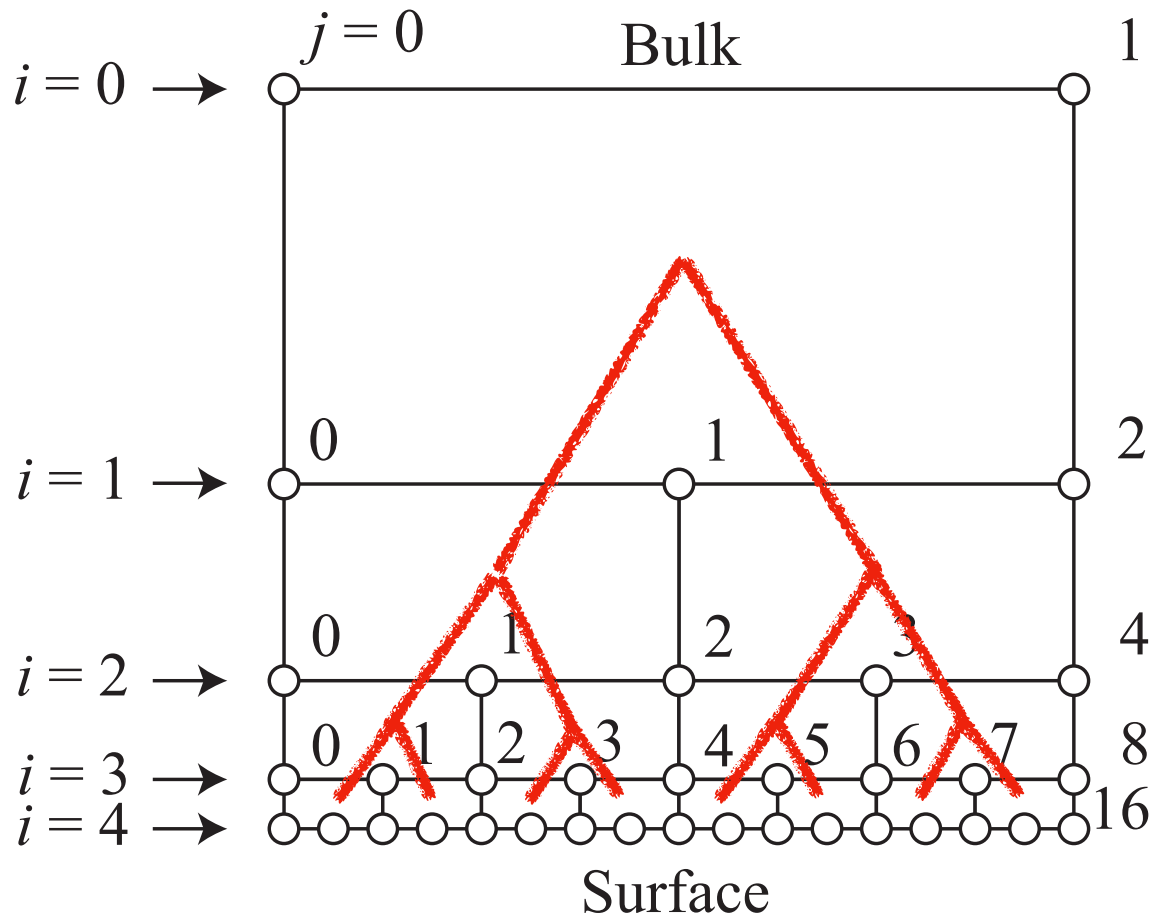
arXiv: [2403.15829](https://arxiv.org/abs/2403.15829)



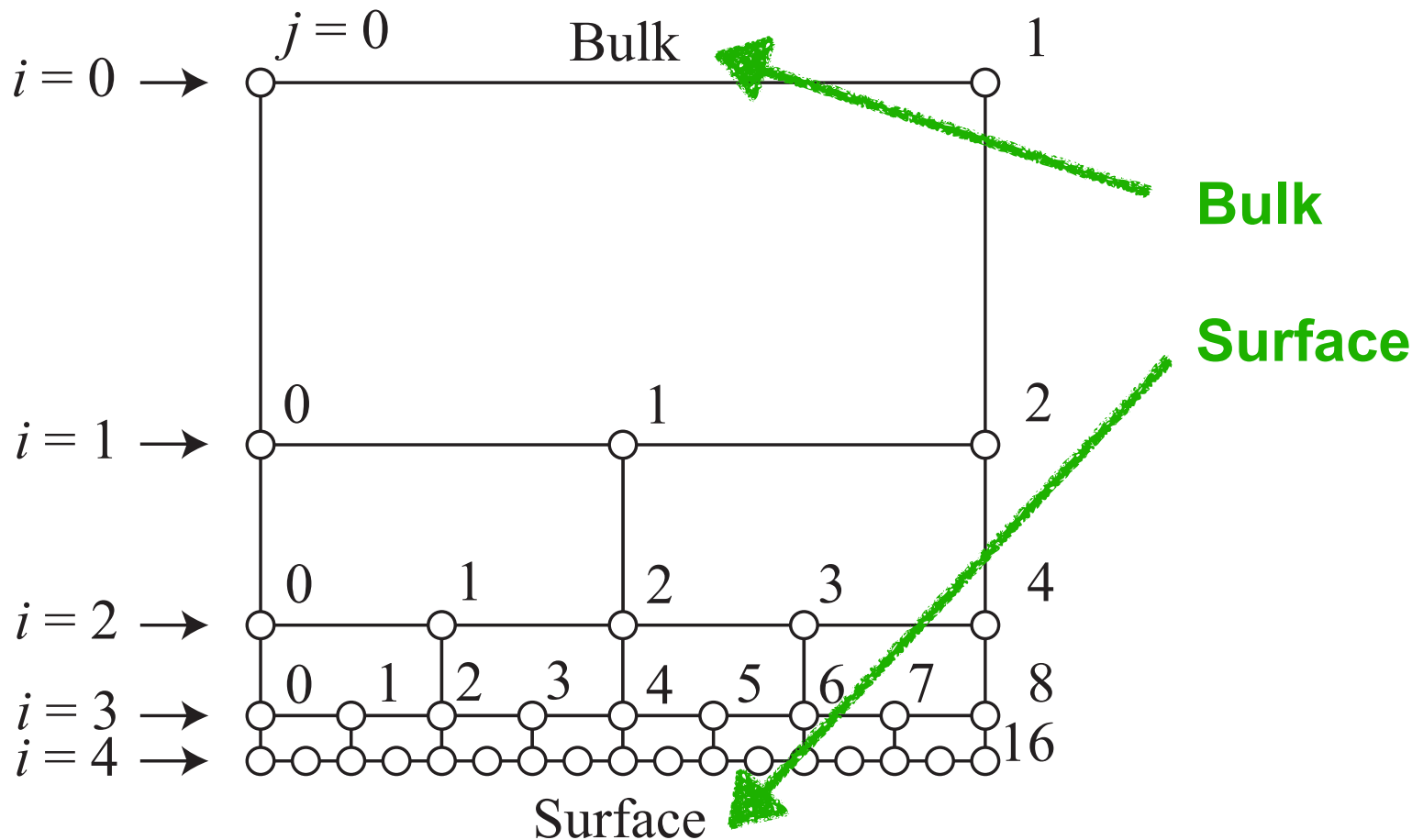
**Pentagons
are stacked!**

**Consider
the Ising Model
on the lattice**

Connecting the center of adjacent pentagons one obtains the Cayley Tree



$$H_n(\{\sigma\}) = -J \sum_{i=0}^n \sum_{j=0}^{m(i)-1} \sigma_j^i \sigma_{j+1}^i - J \sum_{i=0}^{n-1} \sum_{j=0}^{m(i)} \sigma_j^i \sigma_{2j}^{i+1},$$



a variant of CTMRG can be applied to this system

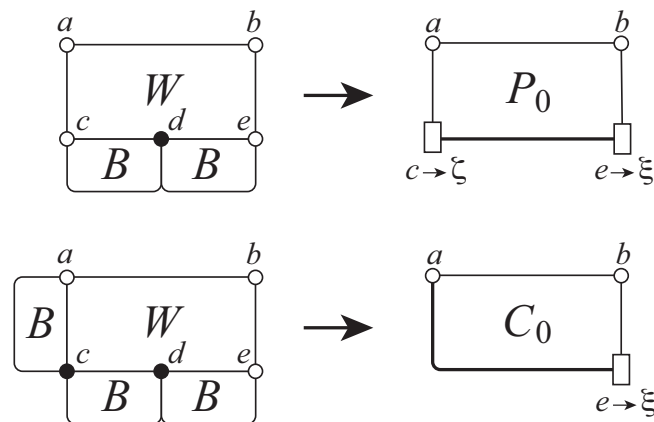


Fig. 7. The smallest HCTM $P_0^{ab}_{\zeta\xi}$ in Eq. (20) and the CTM $C_0^{ab}_{\xi}$ in Eq. (21), which are located around the bottom of the system. Those contracted tensor legs are shown by the filled marks.

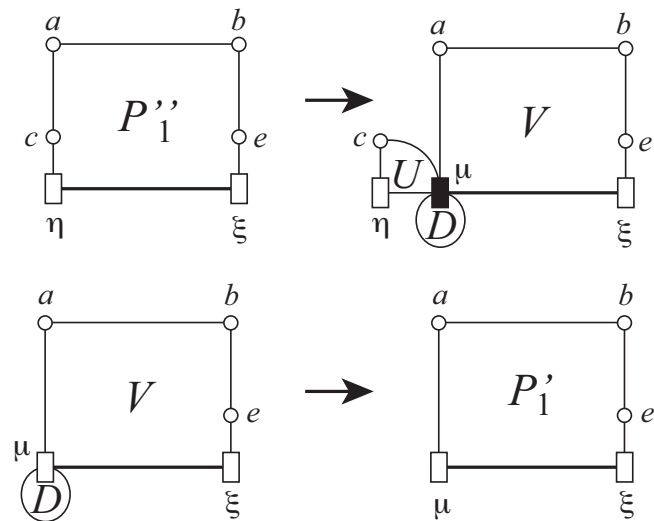
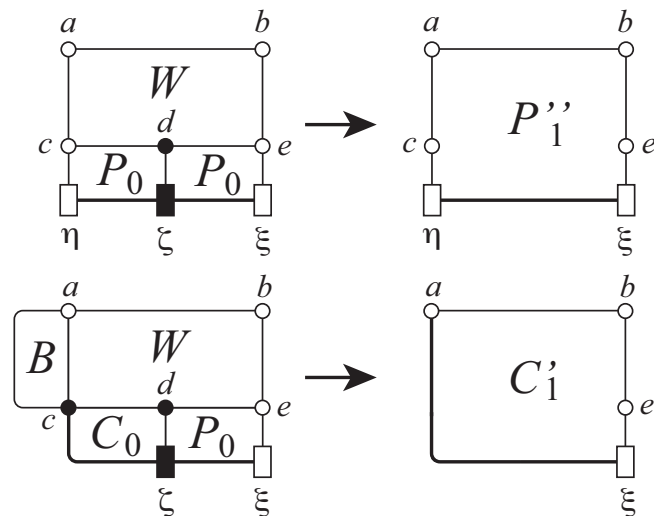
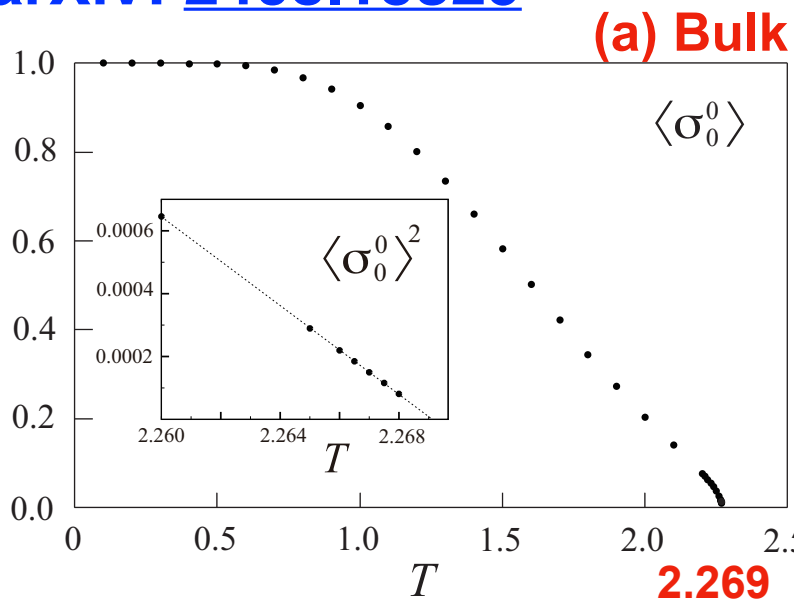


Fig. 9. The SVD in Eq. (25) and the basis transformation applied to P''_1 in Eq. (27).

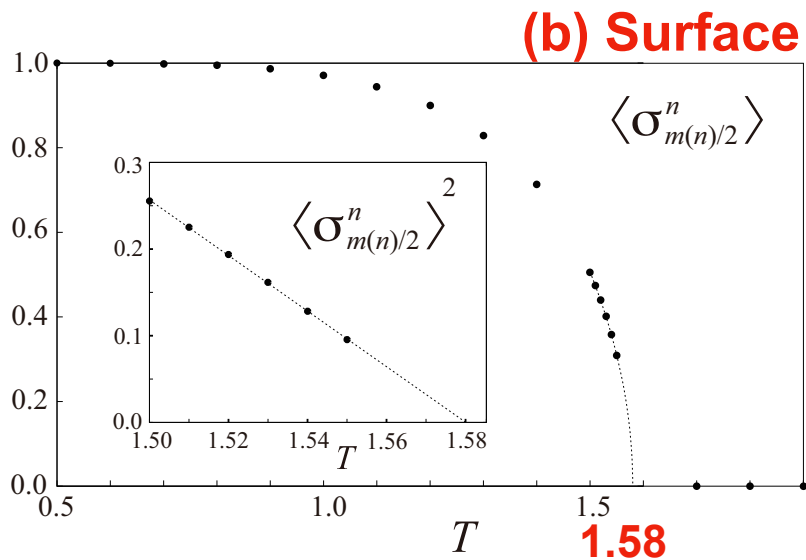
IRF type CTMRG

Eqs. (23) and (24). The extended CTM around the right corner $C'_1{}^{ab}_{c\eta}$ can be obtained in the same manner. We do not have to explicitly calculate it, since the symmetry of the lattice allows us to use C'_1 in Eq. (24) for the bottom right corner, after the appropriate swap of indices.

We have put dash marks on P'_1 and C'_1 in order to indicate that they have more tensor legs, respectively, compared to P_0 and C_0 .



b. Spontaneous magnetization $\langle \sigma_0^0 \rangle$ in the bulk. The square $\langle \sigma_0^0 \rangle^2$ is in the inset.



Bulk-Surface

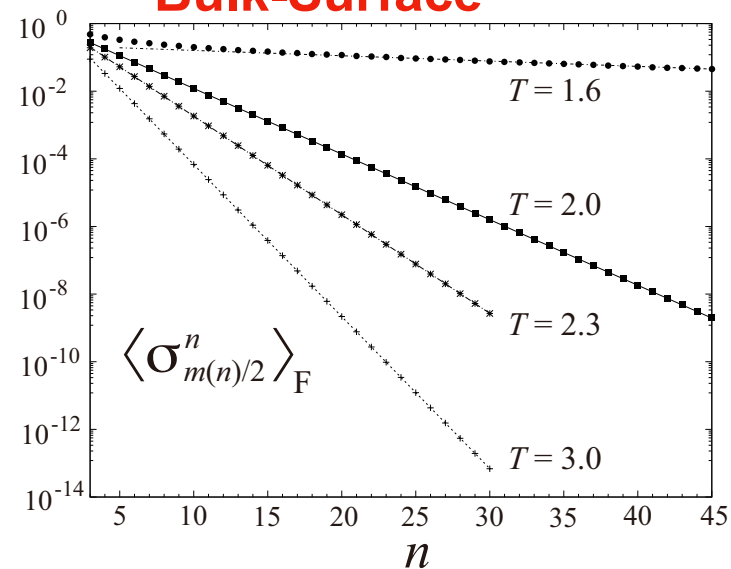
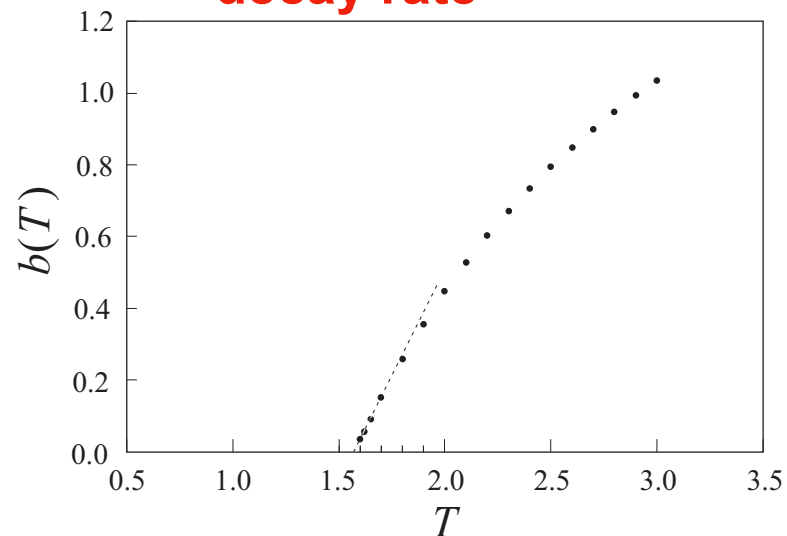
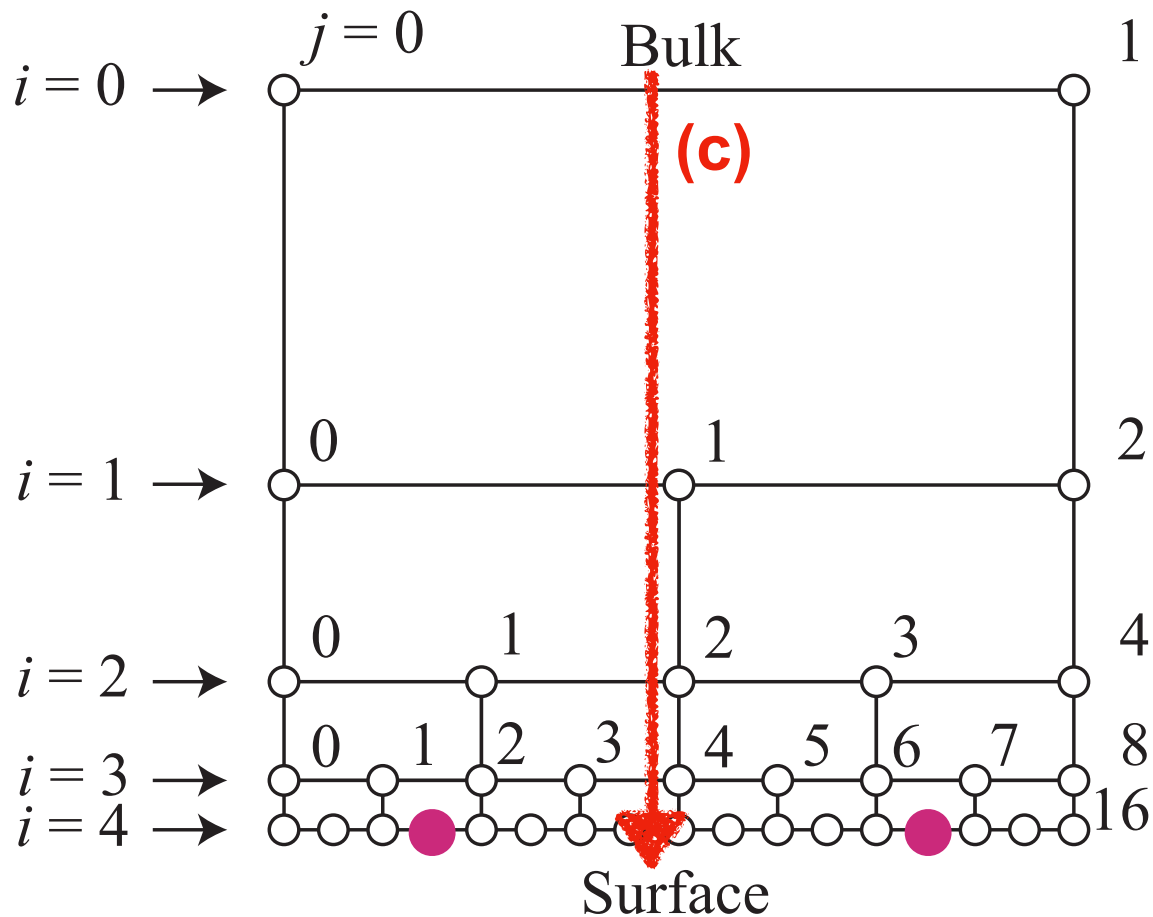


Fig. 15. Decay of $\langle \sigma_{m(n)/2}^n \rangle_F$ with respect to n .

decay rate

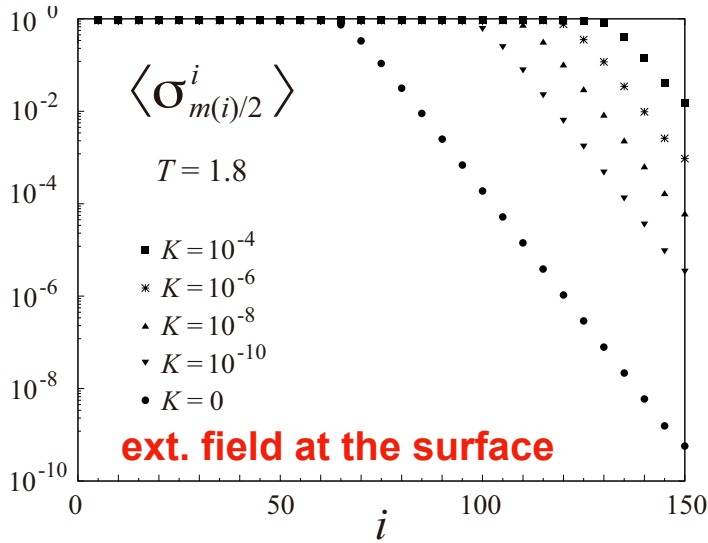


$$H_n(\{\sigma\}) = -J \sum_{i=0}^n \sum_{j=0}^{m(i)-1} \sigma_j^i \sigma_{j+1}^i - J \sum_{i=0}^{n-1} \sum_{j=0}^{m(i)} \sigma_j^i \sigma_{2j}^{i+1},$$



Correlations

(d) Surface



The expectation values $\langle \sigma_{m(i)/2}^i \rangle$ from $i = 5$ to $i = 150$ that are for the system with $n = 150$ layers when $T = 1.8$.

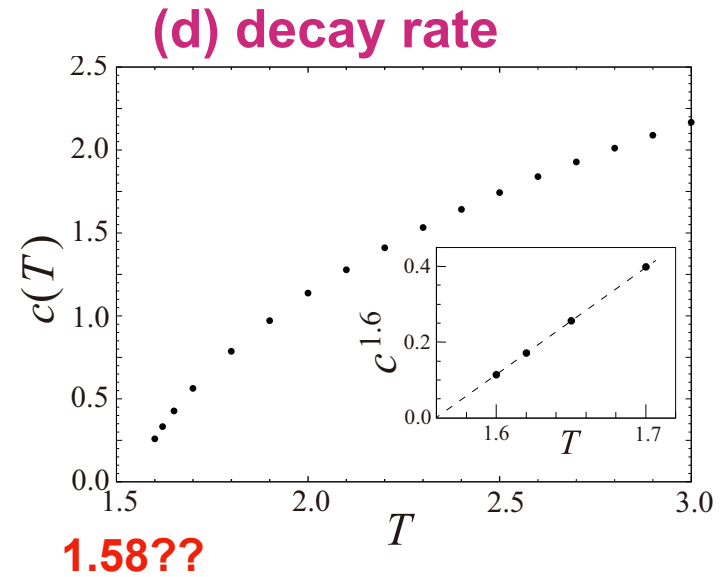
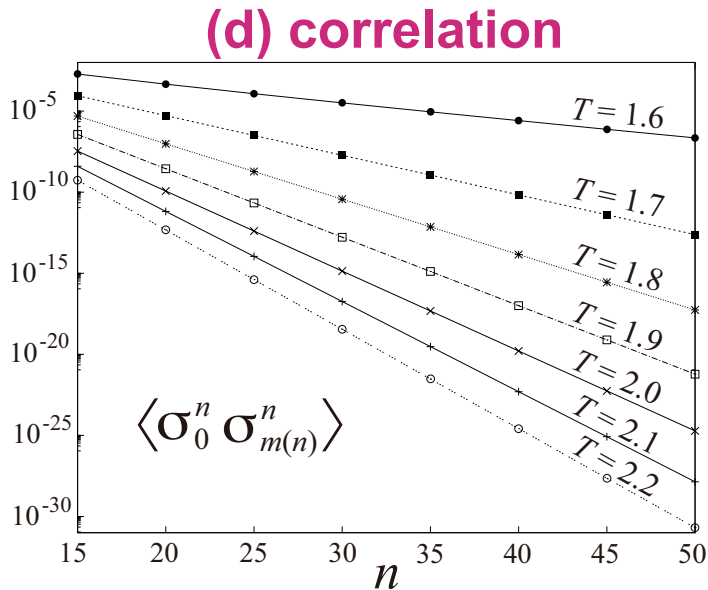


Fig. 19. Temperature dependence of the exponent $c(T)$ in Eq. show $[c(T)]^{1.6}$ neat $T = T_1$ in the inset.

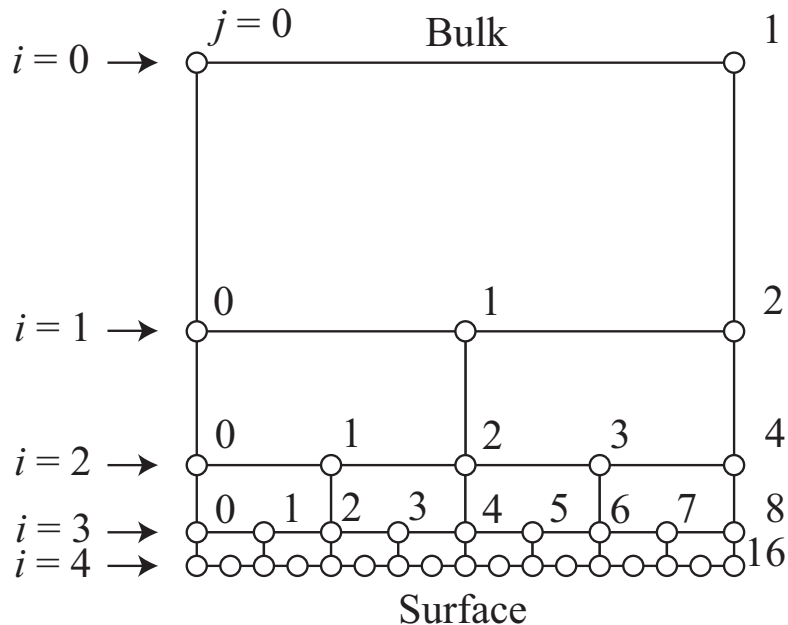
Finally, let us examine how strongly σ_0^n and $\sigma_{m(n)}^n$ related, observing the expectation value $\langle \sigma_0^n \sigma_{m(n)}^n \rangle$ for field case $K = 0$. Figure 18 shows the calculated results for $T = 1.6$ to $T = 2.2$ by the step $\Delta T = 0.1$, with respect to n . The exponential dumping

$$\langle \sigma_0^n \sigma_{m(n)}^n \rangle \propto e^{-c(T)n}$$

is clearly observed, where $c(T)$ is the dumping constant. It should be noted that the distance ℓ between σ_0^n and $\sigma_{m(n)}^n$ measured along the surface is $m(n) = 2^n$. From the relation

$$\ell^{-\eta} = (2^n)^{-\eta} \propto e^{-c(T)n}$$

application to the Stacked Pentagon lattice



Bulk: $T=2.269$

Surface: $T=1.58$

Mean-field Type transitions

Discussions

- How to consider the continuum limit?
- Variants of the lattice on Hyperbolic Surface?
- Can be defined in any dimension?
- effect of randomness ...